Gill proteome networks explain energy homeostasis during salinity stress in *Oreochromis mossambicus*

Larken Root[1] and Dietmar Kültz[2]

[1]University of Washington
[2]University of California Davis

March 1, 2023

Abstract

Acclimations of *Oreochromis mossambicus* to hypersalinity were conducted with multiple rates of salinity increase and durations of exposure to determine the rate-independent maximum salinity limit and the incipient lethal salinity. Quantitative proteomics of over 3000 gill proteins simultaneously was performed to analyze molecular phenotypes associated with hypersalinity. For this purpose, a species- and tissue-specific data-independent acquisition (DIA) assay library of MSMS spectra was created. From these DIA data, protein networks representing complex molecular phenotypes associated with salinity acclimation were generated. *O. mossambicus* was determined to have a wide "zone of resistance" from approximately 75g/kg salinity to 120g/kg, which is tolerated for a limited period with eventual loss of organismal function. Crossing the critical threshold salinity into the zone of resistance corresponds with blood osmolality increasing beyond 400 mOsm/kg, significantly reduced body condition factor, and cessation of feeding. Gill protein networks impacted by hypersalinity include increased energy metabolism, especially upregulation of electron transport chain proteins, and regulation of specific osmoregulatory proteins. Cytoskeletal, cell adhesion, and extracellular matrix proteins are enriched in networks that are sensitive to the critical salinity threshold. Network analysis of these patterns provides deep insight into specific mechanisms of energy homeostasis during salinity stress.

Title: Gill proteome networks explain energy homeostasis during salinity stress in *Oreochromis mossambicusAuthors*: Larken Root[1] and Dietmar Kultz[1] *Author affiliations*:[1]Department of Animal Sciences, University of California Davis, Meyer Hall, One Shields Avenue, Davis, CA 95616, USA***Keywords****:*quantitative proteomics; DIA assay library; systems biology; fish gill; mass spectrometry; osmoregulation

Abstract:

Acclimations of *Oreochromis mossambicus* to hypersalinity were conducted with multiple rates of salinity increase and durations of exposure to determine the rate-independent maximum salinity limit and the incipient lethal salinity. Quantitative proteomics of over 3000 gill proteins simultaneously was performed to analyze molecular phenotypes associated with hypersalinity. For this purpose, a species- and tissue-specific data-independent acquisition (DIA) assay library of MSMS spectra was created. From these DIA data, protein networks representing complex molecular phenotypes associated with salinity acclimation were generated. *O. mossambicus* was determined to have a wide "zone of resistance" from approximately 75g/kg salinity to 120g/kg, which is tolerated for a limited period with eventual loss of organismal function. Crossing the critical threshold salinity into the zone of resistance corresponds with blood osmolality increasing beyond 400 mOsm/kg, significantly reduced body condition factor, and cessation of feeding. Gill protein networks impacted by hypersalinity include increased energy metabolism, especially upregulation of electron transport chain proteins, and regulation of specific osmoregulatory proteins. Cytoskeletal, cell adhesion, and extracellular matrix proteins are enriched in networks that are sensitive to the critical salinity threshold. Network analysis of these patterns provides deep insight into specific mechanisms of energy homeostasis during salinity stress.

Statement of significance:

The significance of this research is chiefly in determining the applicability of current theory of stress responses. Energy Homeostasis Theory has been developed and applied most often in the context of thermal tolerance, and studies examining osmotic stress have often been done in invertebrates which do not control body fluid osmolality. As such, it is unclear if the theoretical framework accurately describes the response of teleosts to hypersalinity, and whether biological indicators of crossing the critical threshold are useful. This study identifies key evidence for unique stress tolerance zones, and leverages powerful quantitative proteomics tools to describe the molecular phenotype in these zones. This information is valuable in understanding the impacts of salinity on teleost fish. It can be used to determine the level of salinity stress that individuals experience in the field.

Introduction:

Abiotic factors are key determinants of suitable habitat for teleost fish [1]. Fish living in freshwater and brackish systems often have limited migration options due to geographic constraints. Habitat shifts include exploration of areas that vary in salinity, e.g., brackish coastal areas and salt lakes. Euryhaline tilapia regularly occupy freshwater environments but these fish also venture into extremely hypersaline habitats which can exceed 100g/kg in salinity [2], [3]. Salinity tolerance is dependent not only on the salinity of exposure, but also the rate of salinity increase, the ionic composition of saline water, and time and frequency spent at high salinity. Acute salinity challenges involving direct transfer from freshwater to a target salinity are common in environmental physiology research [4]–[7], but acute salinity tolerance is often lower than the salinity to which a fish can acclimate over time and may not represent an ecologically relevant salinity challenge. For example, *O. mossambicus* cannot survive direct transfer from freshwater to seawater (SW) [8], but can be experimentally acclimated to several times SW salinity. Survival for different lengths of time from days to weeks has been used as indicatory of long term survival [9]–[13], despite evidence that degeneration of biological function and mortality can occur in *Oreochromis* species following longer time periods in hypersaline conditions [14].

Energy homeostasis theory provides a framework for understanding the relationship between the intensity of a stress and the duration of exposure using a tiered system of biological function. Within the "optimum" range of an environmental parameter, a basal amount of energy is required to maintain internal homeostasis [15]. In the "pejus" range, energy demand increases linearly with the intensity of the stressor to maintain homeostasis and manage the impacts of stress-related macromolecular damage. The "pessimum" range is reached when energy expenditure and macromolecular damage increase in a non-linear relationship with the stress until loss of function (death). The boundary between pejus (zone of tolerance) and pessimum (zone of resistance) ranges is called the "critical threshold" or the incipient lethal level [16]. Stressor levels in the pejus range are tolerable for long periods but result in reduced reproduction and/or growth due to energy reallocation to stress responses. The pessimum range is only temporarily survivable and will eventually result in death if conditions do not improve [15]. Biological function will cease after crossing the critical salinity threshold, i.e. the Critical Salinity Maximum (CS_{MAX}), if conditions do not improve. Energy homeostasis theory was developed predominantly in the context of thermal stress [17], with the critical threshold defined physiologically by a transition to partial anaerobic metabolism. This indicator may not apply to salinity stress and other physiological indicators of fish transitioning from pejus to pessimum salinity ranges are not yet defined.

Indicators of this transition may be found in whole organism physiology and/or tissue-specific analysis of the interactions of molecular components. Proteomic analysis is a particularly promising approach for this purpose because proteins are linked directly to specific genomic loci via their accession numbers [18] and they define the structures and enact the majority of biochemical processes of each level of biological function [19]. Proteins are thus the primary source of phenotypic variability enabling natural selection [20], [21]. Careful choice of environmental challenges and time points allow the capture of protein signatures, which provide systems-level insight of organismal adaptation to biological function maintenance [22], [23]. In the current study, Data-Independent Acquisition Liquid Chromatography Mass Spectrometry (DIA-LCMS2) was used

to capture gill protein signatures at key points in the salinity-level x duration matrix. Gills are one of the most important sites of fish osmoregulation, in addition to their roles forrespiration, acid-base regulation, and nitrogenous waste excretion [24]. The hypothesis driving this study is that pejus and pessimum ranges of salinity tolerance can be identified based on physiological assessments and corresponding changes in dynamic gill proteome networks.

Methods:

Challenges to "Loss of Escape Response" and short-term acclimation

All experimental procedures were conducted with the approval of the UC Davis IACUC under protocols 20007 and 21846. Two adult *Oreochromis mossambicus* female-male pairs (4 adults total) were bred, and fertilized eggs from the two brood groups incubated in separate tanks. Following hatch, fish were raised for 6 months before the start of acclimation experiments, and all acclimations started before fish were eight months post-hatch. Fish were grown in a 200L tank system in dechlorinated Davis, California tap water, as previously described [25] until used for experiments. In all acclimations, two tanks containing fish from each brood group were used as replicates for a total of 4 tanks per treatment. Two acclimation protocols were used to determine CS_{MAX} , and two additional protocols used to collect samples at relevant salinity-level/duration points before loss of organismal function, defined as Loss of Escape Response (LER, see below)(Supplementary figure 1). In each case salinity was increased once every 24h. To determine CS_{MAX} and impacts of salinity stress, salinity was raised at five different rates of change per day (32, 24, 12, 8, and 6g/kg/day). To determine CS_{MAX} over time at hypersalinity, salinity was increased at a rate of 6g/kg/day to three target salinity levels (85, 95, and 105g/kg) followed by continuous exposure at target salinity until LER. To assess physiological and molecular function at hypersalinity before LER, salinity was raised to four target levels (21g/kg, 55g/kg, 85g/kg, and 105g/kg), with rate adjusted to reach the target after 14 days and samples collected following 24 hours at the final salinity. The 14-day period was chosen such that none of the treatments were impacted by acute salinity stress from too-rapid salinity increase. Finally, to assess the long-term impacts of hypersalinity at just below the critical salinity threshold, fish were acclimated from FW to 75g/kg at 6g/kg/day over 14 days followed by maintenance at the final salinity for 10 weeks for a 12 week acclimation in total. The level of 75g/kg for the final acclimation was determined based on the results from the two acclimations to CS_{MAX}.

All acclimations except the long-term 75g/kg treatment were conducted by increasing salinity via adding saturated brine solution (200g/kg) made from synthetic sea salt (Instant Ocean). Brine was added during daily 10% volume water changes to achieve the appropriate salinity increase to within 0.1g/kg as determined using a portable conductivity meter on salinity mode (TWT Cond 3310 meter, TetraCon 325 probe). At salinities above 60g/kg, 5mL of ammonia/nitrite detoxifier solution (Kordon AmQuel) was added daily to maintain low ammonia and nitrite levels due to reduced biological filtration efficiency. Fish were kept in 30L tanks at 27°C ± 1° on three-tiered racks with treatments randomly distributed to avoid biasing results from increased stress near walking paths [26], differences in light levels, or order of feed distribution. Controls were held in equal volume tanks in FW for 14 days and handled in the same fashion. Fish were fed *ad libitum* in the morning three hours after lights-on in the vivarium on a formulated tilapia floating pellet diet (35% Hi Production Tilapia Food, Star Milling Company), recording total number of pellets added. Following 30 minutes of undisturbed feeding time, remaining pellets were retrieved using a dip net and counted.

For the twelve-week acclimation at 75g/kg salinity, an alternate tank set-up was needed because nitrifying bacteria efficiency in biological filters was significantly reduced in salinities above 60g/kg [27]. A recirculating system was constructed with 30L experimental tanks with overflow outlets sitting inside a larger (400L) tank and a 200L sump containing a flow-through bed of ceramic ring filter media (approx. 15L volume) and protein skimmer (BubbleMagus Curve 7). This allowed for consistent tank size between all acclimations but with a greatly expanded water volume (600 L) and biological filter capacity (biofilter volume of 15L versus 0.5L per tank) which kept ammonia and nitrite levels below 0.25 ppm without the need for additional detoxifying solution. To accurately quantify feeding, pellets were weighed before adding to tanks. Following a 30-minute undisturbed feeding period, feed was retrieved and oven dried at 105°C until weight became constant (approx.

3 hours). Natural pellet dissolution was determined for 10g of feed placed in a 30L tank without fish and treated in the same manner. Treatment tanks reached the final salinity after two weeks, at which time three fish from each tank were euthanized after visually selecting one large, one median, and one small fish and samples acquired to determine blood osmolality before long term acclimation. To determine weight gain, the remaining 12 fish were removed using a dip net from tanks and placed in a pre-weighed 2L pitcher containing water from the tank, final weight recorded, and fish then returned to the tank. This process was repeated every two weeks until the end of the experiment.

Sample collection

At the time of sample collection, fish were removed one at a time from the tank and quickly euthanized [28]. The caudal peduncle was severed and blood collected in non-heparinized capillary tubes and transferred to 0.5mL centrifuge tubes. Tubes were kept at room temperature (RT) for 30 minutes to allow for blood clotting and then centrifuged for 10 minutes at 1000g. Serum was removed to labelled 0.5mL centrifuge tubes and stored at -80°C. Fish were then weighed and total length recorded. Gill epithelium was scraped off with a slide coverslip, placed in aluminum foil, snap-frozen in liquid nitrogen, and placed in -80°C storage. Blood serum osmolality measurements were made using undiluted serum when possible, and diluted with pure water (Optima LC/MS Grade, Fisher Chemical) when necessary due to low volume, with osmolality readings multiplied by the dilution ratio. Osmolality was determined using a freezing-point micro-osmometer (Advanced Instruments model 3300).

Sample processing for proteomics

Seven treatments were chosen to capture states near the critical salinity threshold. Eight samples from each treatment were taken from the short-term 85g/kg and 105g/kg treatments and corresponding FW control, and from the long-term 75g/kg treatment and FW control. Six replicates were sampled from the acclimation to LER at 85g/kg and 105g/kg. Extraction, in-solution trypsin digestion of proteins, and peptide separation using a nanoAcquity UPLC system equipped with Symmetry trap and 250 mm x 1.7µm particle size BEH C18 columns were performed as previously reported [29].

Data Dependent Acquisition (DDA) proteomics

DDA spectra were acquired with an Impact II (Bruker), peak lists generated with DataAnalysis 4.4 (Bruker), and peptide to spectrum matches identified with PEAKS suite X plus (Bioinformatics Solutions Inc., Waterloo, Canada) and X!Tandem Alanine (The GPM) using the*O. niloticus* proteome database downloaded from NCBI RefSeq on Feb. 25, 2020, supplemented with known *O. mossambicus* protein sequences using previously described parameters [29]. Mass tolerance limits were set at 10 ppm for precursors and 0.03 Da for fragment ions. All DDA data and metadata are available at MassIVE (MSV000085745) and ProteomeXchange (PXD020364).

Raw spectral library and DIA assay library construction

An *O. mossambicus* gill spectral library was generated using the peptide-to-spectrum matches and protein annotations from DDA data as previously described [30] to create a non-redundant raw library of MS2 spectra. The initial target list of proteins was filtered using multiple QC criteria to reduce the number of transitions, precursors, peptides, and proteins to a unique set which provided the highest diagnostic value for quantitation. Transitions for the initial target list were chosen automatically from library spectra using Skyline transition settings based on the following criteria: ion 3 to last ion -1; fragment ion charge 1; precursor charge range $1 - 5$; MSMS mass accuracy threshold within 20 ppm of the expected mass. This initial target list was filtered in seven sequential steps using Skyline following a previously published method [31]. The complete assay library including all relevant metadata and corresponding data for the sample training set is available at Panorama Public (https://panoramaweb.org/lr03.url). This assay represents a tier two assay [32].

Data Independent Acquisition (DIA) and statistical analysis

Each sample was analyzed by a second acquisition run using data independent (DIA) mode. LC separation parameters and conditions were identical to those used for DDA but only MS2 spectra were acquired. The DIA mass range was set to 390 – 1015 m/z at 25 Hz scan rate with an isolation width of 10 m/z (0.5 m/z overlap, 2.5 sec scan interval). Quantitative analyses and visualization of DIA data was performed using Skyline 20.0 [30]. At least four (generally six) transition peaks were detected for each peptide and their Q value scored using mProphet and decoys generated by Skyline. The minimal mProphet detection Q-value for peak quality was set to 0.01. MSstats 3.1 [33] was used for power analysis to calculate the fold-change (FC) cutoff that was appropriate for each experiment, as well as statistical significance of differences between treatment and control. The cutoff for multiple testing adjusted p-values [34] was set to $p<0.05$. MSstats analyses were normalized by equalizing medians at a minimum confidence interval of 95% using protein quantity as the scope for the analysis. All DIA data can be accessed at PanoramaPublic (https://panoramaweb.org/lr03.url) and ProteomeXchange (PXD029254).

STRING analysis

Protein-protein interaction networks were produced using STRING ver. 11.0 [35] (*https://string-db.org/*) for important groups of significant proteins, including those significantly regulated in all treatments. Lists of accession numbers for these significant proteins were entered in the search function "multiple proteins", creating network maps and enrichment values as over-representation of network nodes (proteins) with high or low FC in STRING functional clusters, Uniprot keywords, and Pfam, InterPro, or SMART protein domains with a false discovery rate (FDR) <0.05 after correcting for multiple testing using the Benjamini-Hochberg procedure.

Results:

Salinity Tolerance

Non-lethal endpoints indicative of a fish approaching a moribund state are necessary to avoid unnecessary physical distress to animals and for the collection of useable tissue samples. A preliminary experiment conducted with six individuals acclimated using a continuous increase of 6 g/kg/day indicated that loss of equilibrium (LOE), a common endpoint for stress tolerance, did not precede more severe impacts including pronounced lethargy, cessation of feeding, and death. Therefore, we aimed to establish a more humane and consistent endpoint indicative of severe stress. The most consistent behavior was found to be non-reactivity to a potential threat, specifically a dip-net. Normally functioning fish will evade capture in a net, and though many fish appear to move less frequently under salinity stress, they still approach food pellets and avoid nets. When *O. mossambicus* no longer evades the net, this was the most consistent indicator that they will very soon become moribund, and for this reason we introduce the term "Loss of Escape Response" (LER) as an alternative and more humane endpoint to LOE. Two fish in the preliminary experiment which reached LER were rescued, showing that this state is not terminal if the salinity stress is ameliorated. In trials with an LER endpoint, constant fish monitoring allowed for capture of fish before death as this was necessary for acquiring usable serum and tissues for proteomics.

High rates of salinity increase induced acute effects, resulting in lower CS_{MAX} than rates below 12g/kg/day (Table 1). Based on the CS_{MAX} for the 8 g/kg/day and 6 g/kg/day rates the acclimatory CS_{MAX} is approximately 115g/kg for this population and experimental set-up. This result defines the upper end of the pessimum salinity range. For long-term challenges, decreasing increments of 10g/kg lower than the CS_{MAX} (115g/kg) were used until a salinity was found in which fish were able to survive indefinitely to determine the critical salinity threshold. The mean times until LER at these salinity levels were as follows: 263 hours at 105g/kg, 326 hours at 95g/kg, and 559 hours at 85g/kg (Table 1). 79% of individuals survived at 75g/kg for 10 weeks.

Whole organism physiology

Blood osmolality

Blood osmolality data were collected for all treatments at LER in all experiments (Figure 1A). Blood

osmolality was significantly higher ($p < 0.05$) for all treatments compared with control except 21g/kg and 55g/kg. Blood osmolality was 810 mOsm ± 92.6 at LER for the 85g/kg treatment and 797 mOsm ± 107.7 at LER for the 105g/kg treatment, both significantly higher ($p < 0.05$) than short-term and long-term FW handling controls. Blood osmolality was 389 mOsm ± 19.1 following 10 weeks at 75g/kg, and 353.9 mOsm ± 6.38 for the handling control. Following 24 hours after acclimation to 75g/kg in this experiment, blood osmolality was 399 ± 19.2. Acute salinity stress following transfer to 32g/kg increased blood osmolality to 655 mOsm ± 20.8 at LER (n=8).

Body condition

Fulton's body condition factor (K) was calculated for fish following the 14-day acclimation and the extended constant salinity treatments (Figure 1B). K was significantly lower (2.79 *vs.* 3.12, $p = 0.013$) for the 105g/kg acclimation compared with handling controls. For long-term exposure to LER, K was 2.67 ± 0.173 for the 85g/kg treatment and 2.53 ± 0.415 for the 105g/kg treatment, both of which were significantly lower ($p < 0.05$) versus short-term and long-term FW handling controls. Following 10 weeks at 75g/kg, K was 2.98 ± 0.264, K for handling controls was 3.05 ± 0.242, and K following 24-hours at 75g/kg was 3.16 ± 0.376.

Feeding and Growth

During short-term acclimations, feeding was similar for FW controls, fish at 21g/kg, and at 55g/kg. Feeding decreased for both the short-term and long-term 85g/kg and 105g/kg treatments with complete cessation of feeding as the target salinity was reached. At 75g/kg, feeding dropped to near zero during the initial acclimation period but recovered to near the feeding rate of the handling control, although at end of the experiment feeding was still significantly lower ($p = 0.0093$) than the control (Figure 2C). Growth was measured biweekly only for the 75g/kg extended salinity experiment (Figure 2B). Control and treatment diverged significantly in weight after two weeks at 75g/kg (week 4 weighing). No significant growth was measured for the 75g/kg treatment from the time of reaching the final salinity until the end of the experiment. Overall, mean weight increased by 37% from the original weight in the 75g/kg treatment over 12 weeks from 3.756 g/fish to 5.173 g/fish. In comparison, the control treatment increased by 214% of the original weight from 3.933 g/fish to 12.37 g/fish.

DIA quantitative proteomics

Construction of the DIA assay library

The raw MS2 spectral library from data-dependent acquisition (DDA) LCMS2 data of all samples contained 16,306 proteins, 139,790 peptides, 154,426 precursors (different charge states of peptides), and 864,374 transitions (fragment ions) (Supplementary fig. 2). Applying the quality control (QC) filter steps resulted in a final DIA assay library comprised of a target list containing 68,586 transitions, 13,847 precursors (one per peptide), and 3024 proteins. Despite requiring each protein to be represented by at least two unique peptides in the raw spectral library, 27.3% (825) of the proteins are only represented by a single peptide (although multiple transitions) in the final DIA assay library because other peptides were excluded during DIA assay library construction if they did not meet the QC criteria in all filter steps.

Proteome regulation during salinity stress

Proteomic analysis was performed for seven treatments using the same DIA assay library. The mass error threshold was <20 ppm for all transitions in all samples and <10 ppm for the great majority, and retention time reproducibility of the data was very high as well (Supplementary fig. 3). A fold-change (FC) threshold of 2.0 was enforced for all treatments in considering statistical significance based on the coefficient of variation calculated with MSstats [33], providing at least 0.8 statistical power for p-values <0.05. Furthermore, the majority of transition peaks for all samples in this dataset had mProphet [36] peak scores of q<0.01, the peak quality threshold for inclusion in MSstats quantitative DIA data analysis.

Short-term acclimation to 85g/kg resulted in 234 significantly upregulated and 171 significantly downregulated out of 2971 total proteins quantified, while acclimation to 105g/kg yielded 348 significantly upregulated

and 255 significantly downregulated out of 2972 total proteins quantified (Figure 3A, Supplementary table 1). Exposure to LER resulted in 501 significantly upregulated and 481 significantly downregulated out of 3015 proteins quantified at 85g/kg, and 486 significantly upregulated and 473 significantly downregulated out of 3015 proteins quantified at 105g/kg. Long-term acclimation at 75g/kg resulted in 311 significantly upregulated and 149 significantly downregulated out of 3011 proteins quantified.

The top five most highly upregulated and downregulated significant proteins based on FC were determined for each treatment and compared between treatments (Figure 3B). The most highly upregulated protein in all extended treatments and the second most highly upregulated in the short-term acclimations was inositol monophosphatase 1 isoform X1 (IMPase1-X1), which had a maximum upregulation in the extended 85g/kg salinity treatment of 438 FC and an average FC increase of 225 across all five treatments. Solute carrier family 12 member 2 isoform X1 (SLC12a2-X1) was the highest upregulated protein in both short-term acclimations and the second most highly upregulated protein in the extended treatments, with an average FC of 90 times greater across all treatments. The most highly downregulated protein in four of the five treatments was an uncharacterized protein, LOC100699110 isoform X1, which was 1137 times lower in the extended 105g/kg exposure and 513 times lower on average across all treatments.

There was a large degree of overlap in significantly regulated proteins in each treatment (Figure 3C). The greatest number of shared proteins was between samples taken at LER, with 472 of the significantly regulated proteins shared between the extended exposure at 85g/kg and at 105g/kg. The second largest group of overlapping proteins were those which were significantly regulated in all treatments, including 161 proteins. The extended salinity treatments each had many proteins which were only significantly regulated in one treatment, with 144 uniquely significant proteins in the 85g/kg salinity, 110 in the 105g/kg salinity, and 87 in the 75g/kg salinity. A total of 78 proteins were significantly regulated in all four treatments above the critical salinity threshold.

Network analysis

STRING network for significant proteins in all treatments

A protein network map was created visually representing the response of*O. mossambicus* gill proteins to hypersaline conditions regardless of time of exposure or hypersalinity relative to the critical threshold using all 161 proteins significantly regulated in all treatments. The majority (122) of accession numbers matched to STRING IDs, and 86 were connected to at least one other protein. The network map of all connected proteins contains many proteins involved in the electron transport chain (ETC), with 36 of the 86 total proteins being a subunit of one of the five ETC complexes (Figure 4). Core members of the glycolysis and tricarboxcylic acid (TCA) cycle pathways accounted for another 17 nodes of this network map. Only three of the proteins in the network map were downregulated, Na^+/K^+-ATPase α-1 isoform X4, Alkylglycerone phosphate synthase, and $NH_4{}^+$ transporter Rh-B. One of the clusters which is highly connected included two isoforms of acetyl-CoA acyltransferase, two isoforms of aldehyde dehydrogenase 6-A1, two trifunctional proteins, enoyl-CoA δ isomerase 1, and electron transfer flavoprotein β. Another important set of nodes on this map are the two isoforms of IMPase, one of which was the most highly upregulated protein in many treatments.

STRING networks for pejus and pessimus range physiological states

All treatments 85g/kg and greater represent pessimum range salinities given the ultimate LER endpoint at these salinities. Network analysis was run for the 78 proteins shared by short-term and long-term salinity treatments at 85g/kg and 105g/kg and compared with the networks for the 87 proteins unique to the extended 75g/kg treatment. Networks were identified with greater than three nodes and classified using ontological term enrichment. Pejus range regulation consisted of a network of mostly upregulated proteins with enrichment in amino acid metabolism and oxidoreductase terms including lactate dehydrogenase (LDH) and glycogen synthase, a network of up and down-regulation of structural proteins, especially myosin subunits, and downregulation of proteasome proteins (Figure 5A). Pessimum range networks contained specific upregulated mitochondrial proteins, with subunits in the cytochrome b-c1 complex as central members, and

downregulation of extracellular matrix proteins (ECM) with several collagen subunits (Figure 5B).

Identifying Uncharacterized Protein LOC100699110 - X1

The most highly regulated protein analyzed was an uncharacterized protein given the NCBI accession number XP_019220227.1. Searching the amino acid sequence using NCBI pBLAST found the closest annotated proteins to be fucolectin, pentraxin fusion-like protein, and tenascin (Supplementary fig. 4). Examining the amino acid sequence revealed that protein XP_019220227.1 consists mainly of eleven repeats of 143 amino acids with 94.4% identity between repeats. Searching the repeat sequence on pBLAST returned matches with high identity to fucolectins from different teleost fish with E-values lower than 2E-70 and identity greater than 75%. Matching fucolectins were much shorter, between 147 and 321 amino acids long in comparison with the 1605 amino acid length of the uncharacterized protein.

DISCUSSION

Salinity tolerance

Physiological tolerance limits of fishes to environmental stressors are species-specific and sensitive to time course of exposure. Common assessments of upper salinity limits such as LOE may not be applicable to all species [12]. Therefore, here we introduce an endpoint based on non-reactivity to a dip-net (LER), a threat which all normally functioning fish recognized, to determine approaching morbidity. Several fish in this state were rescued through transfer to improved conditions, suggesting that they were still functional with physiological and molecular phenotypes representative of living individuals, not pre-mortem internal processes.

An exposure protocol was developed to account for salinity level, time of exposure, and rate-of-change. Salinity tolerance is often assessed in a binary fashion between acute exposure i.e. direct transfer from initial to final salinity, and chronic exposure which involves gradual salinity change to the endpoint [12]. These assessments do not fully capture the dynamics of salinity acclimation, as a high rate of salinity change may outpace the necessary alterations in phenotype required for acclimation. Additionally, without duration at a final salinity one cannot assess the breadth of the zone of resistance (pessimum range). Previous assumptions about survival for a specific amount of time representing long term-survivability may be inaccurate, as *O. mossambicus* can survive in salinity above the incipient lethal salinity for up to six weeks.

O. mossambicus has been recorded in nature in salinities up to 120g/kg, with historical data indicating that they can remain in extreme hypersaline conditions for weeks and even months [3]. This data aligns with our results, with fish able to survive for several weeks above 100g/kg, and for months at 75g/kg. Experimental conditions are of course different from natural conditions, and impacts of predator avoidance and foraging can increase the effects of environmental stress [37]. Nevertheless, extreme hypersaline ecosystems have greatly reduced species diversity and thus *O. mossambicus* is likely to experience fewer predators and greater food availability due to fewer competitors [3].

Salinity exposure near the Critical Threshold eliminates growth

Energy homeostasis theory describes survival as the final biological capacity lost when animals are exposed to pessimum range stressors for too long [15]. Fish can sustain life in pejus range levels, but energy demands required for survival, sub-optimal enzymatic function, and/or contending with deleterious effects of increased metabolic processes contribute to reduced growth or reproduction, ultimately reducing the functional capacity of individuals and populations. This was demonstrated clearly through the 12-week exposure to 75g/kg treatment experiment, where most fish were able to survive and maintain blood osmolality, body condition, and feeding rate close to control levels, but growth was dramatically reduced to the point of no significant weight increase.

Absolute salinity and time of exposure each played a role in determining the internal level of stress, i.e. distortion from homeostasis. Physiological parameters such as blood osmolality and body condition were

significantly impacted by extreme hypersalinity with greater change from controls at higher absolute salinity. However, over time the difference between fish held at 85g/kg and 105g/kg was erased when LER was reached, whereas internal levels were maintained at 75g/kg, indicating a clear external salinity threshold based on ultimate outcome. Internal blood osmolality was also higher in fish held at 85g/kg or 105g/kg versus acute exposure to 32g/kg at LER, pointing to a greater acclimatory upper limit of blood osmolality in chronic exposures versus acute salinity change. Protein abundance changes were greatest in fish with significantly higher blood osmolality, providing evidence that gill molecular phenotypes are not a direct result of specific salinity levels or exposure times, but rather that combinations of salinity, time of exposure, and rate of increase lead to different internal states and survival outcomes.

Regulation of protein networks in hypersalinity

The largest and most highly connected cluster in the network of significantly regulated proteins in all treatments included mitochondrial proteins involved in the ETC. Multiple previous proteomic studies with *Oreochromis* species have shown the widespread upregulation of mitochondrial proteins during acclimation to higher salinity levels, especially as these levels approach the upper range of salinity tolerance [29], [38], [39]. Microscopy has shown that ionocytes, the main site of transepithelial ion transport in fish gills [40], increase in number within 12 hours and remain elevated following transfer of *O. mossambicus* from FW to SW [41]. Additionally, SW-specific ionocyte subtypes are significantly larger than ionocytes from fish in FW [42]. Ionocytes, once called mitochondrial rich cells (MRCs) [43], are characterized by high concentrations of mitochondria, which is reflected in protein abundance patterns from this and previous studies.

In addition to ETC proteins, the hypersalinity response network combining all treatments has a strong representation of glycolysis and the TCA cycle proteins, emphasizing the importance of increased energy production in response to hypersaline conditions in initial and long-term stages of exposure. These proteomic responses combined with decreasing body condition/growth indicate that one of the dominant adaptive mechanisms of *O. mossambicus* to hypersaline conditions is to increase energy production and allocation to meet increased osmoregulatory energy requirements. Osmoregulation can account for 20-50% of basal metabolic cost across a range of taxa in fish [44]. Comparing *O. mossambicus* oxygen consumption rates, fish acclimated to hypersaline water at 1.6X SW salinity had higher oxygen consumption than in FW or SW [6]. Evidence is scant for salinity levels as high as those used in this study, but it is reasonable to suggest that increasing hypersalinity requires greater energy devoted to osmoregulation, especially given that much of the active ion transport is ATP-dependent.

Proteins directly related to ion regulation in the network of significant proteins in all treatments, specifically ion transporters (Na^+/K^+ ATPase, NH_4^+ transporter) and compatible osmolyte synthesis enzymes (IMPase, sorbitol dehydrogenase), are present but are peripheral in the network map and do not contain many members. Small numbers of significant proteins combined with a high degree of regulation (many are among the most highly regulated proteins), indicate that ion balance is controlled through highly targeted regulation of specific proteins and subunits. This contrasts with the regulation of energy production, which is comprehensive and involves a large network cluster. Targeted regulation of ion transport includes isoform switching in Na^+/K^+ATPase subunits, as the α-1 isoform X1 increased by an average of 10-fold greater in all treatments while α-1 isoform X4 decreased by 20-fold on average. Isoform switching in Na^+/K^+ ATPase subunit α has been documented in *O. mossambicus* [45] and other fish species [46] during salinity acclimation. In *O. mossambicus* ,*myo* -inositol is synthesized to counteract increased intracellular electrolyte concentration through a two-step metabolic path from D-glucose by the enzymes *myo* -inositol-3-phosphate synthase (MIPS) and IMPase [47], and as stated IMPase 1 isoform X1 was the most highly upregulated protein on average across treatments. MIPS was also significantly upregulated in all treatments except the extended 75g/kg exposure. *Myo* -inositol concentration is also regulated in*O. niloticus* kidney during salinity acclimation, although here the mechanism is to reduce degradation by downregulating*myo* -inositol oxidase[39]. Interestingly, no*myo* -inositol related proteins were significantly regulated by salinity in gills of *O. niloticus,* which has an upper salinity tolerance limit near 25 g/kg [29].

The hypersalinity response network also includes a cluster (Figure 4, inset 2) which includes proteins involved

in fatty acid β-oxidation and detoxification. Acetyl-CoA acyltransferase is involved in producing acetyl-CoA through β-oxidation to be processed in the TCA cycle. Aldehyde dehydrogenase (ALDH) is involved in fatty acid metabolism but also neutralizes carbonyl compounds resulting from lipid peroxidation [48]. Lipid peroxidation is one result of oxidative stress causing turnover in lipid membranes and the formation of toxic fatty aldehydes, which ALDH plays a large role in converting into fatty acids [49]. ALDH was also highly upregulated in *O. niloticus* kidney indicating that this response is conserved across species and tissues [39]. Upregulation of acetyl-CoA acyltransferase has also been observed in other organisms exposed to toxic compounds such as in mice exposed to perflourooctane sulfonate [50], diphenylarsinic acid [51], and in bacteria exposed to hydrocarbon spills [52].

Pejus range protein network regulation

Stress level specific responses fall into two broad categories; upregulation in energy metabolism and variable regulation of structural proteins. Pejus range regulation networks include one with mostly upregulated proteins, many of which participate in amino acid metabolism. Downregulation of the proteasome affects both energy and amino acid metabolism. It reduces protein turnover to redirect energy towards osmoregulation and it may reduce the availability of free amino acids liberated from degraded proteins. As noted earlier, specific markers for passing the critical threshold into the pessimum range during thermal stress may not apply during salinity stress. Thermal stress is predicted to lead to increased lactate through anaerobic metabolism only above the critical threshold [15], whereas our data show upregulation in LDH only occurs in the 75g/kg treatment. Energy demand required in hypersalinity appears to be supplied mainly through oxidative phosphorylation and carbohydrate metabolism with some additional fatty acid β-oxidation. In addition, in the pejus range, amino acid metabolism is significantly affected, which may contribute to the regulation of energy metabolism (e.g. via regulation of gluconeogenesis).

The other major protein network includes structural proteins such as several myosin subunits which are significantly upregulated in pejus range salinities but significantly downregulated in pessimum range salinities. However, tropomyosin β is significantly downregulated in the pejus range and upregulated (n.s.) in the pessimum range. The regulation of structural proteins is further discussed in the following section.

Pessimum range protein network regulation

The energy metabolism protein network associated with the pessimum range consists mainly of upregulated mitochondrial proteins, especially Cytochrome b-c1 complex subunit 7. Structural changes in the pessimum range include downregulation of ECM proteins including collagen subunits, and proteins forming the connection between the ECM and cell membrane, e.g., integrin-α. These proteins are highly responsive to the intensity of salinity stress rather than being uniformly regulated during hypersaline exposure. Structural proteins were a functional category with a high degree of non-linearity in regulation of mRNA and proteins in *O. niloticus* , further indicating that cell structure regulation is complex and likely fluctuates in response to internal and external signaling, especially around the critical threshold.

Tissue structure changes are expected, as *O. mossambicus* has dramatically reduced epithelial permeability as salinities increase above SW [53]. Ionocytes involved in osmoregulation in high salinity environments have unique apical crypts in comparison with other types of ionocytes [54], [55]. In high salinity, ionocytes form clusters [56], and develop a complex microtubule network along their basolateral membrane [57]. The formation of tubulin networks in response to salinity was first noted decades ago in *Cyprinodon variegatus* and *Fundulous heteroclitus* [57], [58]. This provides context for the highly downregulated uncharacterized protein we have identified as fucolectin-like. While the role of lectins is not fully understood in fish physiology [59], they likely play an important role in the regulation of microtubule networks in response to salinity. Binding sites have been identified on exposed fish gill epithelium which interact with the lectins wheat germ agglutinin (WGA), peanut lectin agglutinin (PNA), and concanacalvin A (ConA) [60]. WGA exposure stimulates Ca^{+} ion uptake in *O. mossambicus* in Ca^{+} deficient water and promote microtubule network formation [61]. WGA and PNA only react with FW specific ionocytes in *O. mossambicus* (WGA) [62] and *Oncorhynchus mykiss* (PNA) [63]. The uncharacterized protein, along with rhamnose binding lectin which was also one

of the most highly downregulated proteins in our data set, may be FW specific for *O. mossambicus* , and downregulation may help reduce Ca^{+}uptake. This would help in osmoregulation and impact cell-cell adhesions through cadherin binding, which is also impacted by the high upregulation of δ-catenin 1.

Conclusions

This study presents a novel experimental design for assessment of stress combined with an innovative approach for systems-level analyses of molecular phenotypes (DIA-LCMS2). Specific organismal phenotypes (blood osmolality, body condition, feeding rate) were found to indicate extreme salinity stress in *O. mossambicus* . The rate-independent salinity maximum and critical threshold salinity were determined using a comprehensive set of acclimations and a generalized protocol that is applicable to other species. The DIA-LCMS2 approach was shown to reveal comprehensive molecular phenotypes in ecologically relevant samples. The data generated in this study were used to produce protein networks which elucidate major mechanisms of ionic and mitochondrial protein regulation in response to hypersalinity in general and with respect to the critical threshold. These networks help explain how fish modulate energy metabolism, cell adhesion, and cell structure when experiencing salinity stress below and above the critical limit.

Acknowledgements:

This investigation was supported by the National Science Foundation (NSF-BSF) Grant IOS-2209383 to DK, the US-Israel Binational Agricultural Research and Development Fund (BARD) Grant (IS-4800-15 R) to DK, and AES projects CA-D-ASC-7690-H and CA-D-ASC-7624-RR to DK.

References:

[1] Somero, G., Lockwood, B., Tomanek, L., *Biochemical Adaptation, Response to Environmental Challenges from Life's Origins to the Anthropocene* . Sinauer Associates, an imprint of Oxford University Press, 2016. Accessed: Aug. 12, 2021. [Online]. Available: //global.oup.com/ukhe/product/biochemical-adaptation-9781605355641

[2] J. Panfili *et al.* , "Influence of salinity on the life-history traits of the West African black-chinned tilapia (Sarotherodon melanotheron): Comparison between the Gambia and Saloum estuaries," *Aquat. Living Resour.* , vol. 17, no. 1, pp. 65–74, Mar. 2004, doi: 10.1051/alr:2004002.

[3] A. K. Whitfield, R. H. Taylor, C. Fox, and D. P. Cyrus, "Fishes and salinities in the St Lucia estuarine system—a review," *Rev Fish Biol Fisheries* , vol. 16, no. 1, pp. 1–20, Feb. 2006, doi: 10.1007/s11160-006-0003-x.

[4] M. A. Amoudi, A.-F. M. El-Sayed, and A. El-Ghobashy, "Effects of Thermal and Thermo-Haline Shocks on Survival and Osmotic Concentration of the Tilapias Oreochromis mossambicus and Oreochromis aureus × Oreochromis niloticus Hybrids," *Journal of the World Aquaculture Society* , vol. 27, no. 4, pp. 456–461, 1996, doi: 10.1111/j.1749-7345.1996.tb00630.x.

[5] A. A. Fuadi, I. R. J. Hasly, L. I. Azkia, and M. Irham, "Response of tilapia (Oreochromis niloticus) behaviour to salinity differences: a laboratory scale study," *IOP Conf. Ser.: Earth Environ. Sci.* , vol. 674, no. 1, p. 012060, Feb. 2021, doi: 10.1088/1755-1315/674/1/012060.

[6] G. K. Iwama, A. Takemura, and K. Takano, "Oxygen consumption rates of tilapia in fresh water, sea water, and hypersaline sea water," *Journal of Fish Biology* , vol. 51, no. 5, pp. 886–894, 1997, doi: 10.1111/j.1095-8649.1997.tb01528.x.

[7] B. D. Kammerer, J. J. Cech, and D. Kültz, "Rapid changes in plasma cortisol, osmolality, and respiration in response to salinity stress in tilapia (Oreochromis mossambicus)," *Comparative Biochemistry and Physiology Part A: Molecular & Integrative Physiology* , vol. 157, no. 3, pp. 260–265, Nov. 2010, doi: 10.1016/j.cbpa.2010.07.009.

[8] E. L. Lewis and R. G. Perkin, "Salinity: Its definition and calculation," *Journal of Geophysical Research: Oceans* , vol. 83, no. C1, pp. 466–478, 1978, doi: 10.1029/JC083iC01p00466.

[9] J. Blackburn, "Revised procedure for the 24-hour seawater challenge test to measure seawater adaptability of juvenile," *Canadian Technical Report of Fisheries and Aquatic Sciences* , vol. 1515, 1987, Accessed: Aug. 12, 2021. [Online]. Available: https://ci.nii.ac.jp/naid/10005103917/

[10] E. A. F. Christensen, M. Grosell, and J. F. Steffensen, "Maximum salinity tolerance and osmoregulatory capabilities of European perch Perca fluviatilis populations originating from different salinity habitats," *Conservation Physiology* , vol. 7, no. 1, p. coz004, Feb. 2019, doi: 10.1093/conphys/coz004.

[11] J. N. Langston, P. J. Schofield, J. E. Hill, and W. F. Loftus, "Salinity Tolerance of the African Jewelfish Hemichromis letourneuxi, a Non-native Cichlid in South Florida (USA)," *Copeia* , vol. 2010, no. 3, pp. 475–480, Sep. 2010, doi: 10.1643/CP-09-069.

[12] E. Schultz and S. McCormick, "Euryhalinity in an Evolutionary Context," in *Euryhaline Fishes* , vol. 32, 2012, pp. 477–533. [Online]. Available: https://opencommons.uconn.edu/eeb_articles/29

[13] W. O. Watanabe, C.-M. Kuo, and M.-C. Huang, "The ontogeny of salinity tolerance in the tilapias Oreochromis aureus, O. niloticus, and an O. mossambicus × O. niloticus hybrid, spawned and reared in freshwater," *Aquaculture* , vol. 47, no. 4, pp. 353–367, Aug. 1985, doi: 10.1016/0044-8486(85)90220-0.

[14] B. A. Sardella, "Physiological, biochemical and morphological indicators of osmoregulatory stress in 'California' Mozambique tilapia (Oreochromis mossambicus x O. urolepis hornorum) exposed to hypersaline water," *Journal of Experimental Biology* , vol. 207, no. 8, pp. 1399–1413, Mar. 2004, doi: 10.1242/jeb.00895.

[15] I. M. Sokolova, M. Frederich, R. Bagwe, G. Lannig, and A. A. Sukhotin, "Energy homeostasis as an integrative tool for assessing limits of environmental stress tolerance in aquatic invertebrates," *Marine Environmental Research* , vol. 79, pp. 1–15, Aug. 2012, doi: 10.1016/j.marenvres.2012.04.003.

[16] J. R. Brett, "Some Principles in the Thermal Requirements of Fishes," *The Quarterly Review of Biology* , vol. 31, no. 2, pp. 75–87, Jun. 1956, doi: 10.1086/401257.

[17] H.-O. Pörtner, "Oxygen- and capacity-limitation of thermal tolerance: a matrix for integrating climate-related stressor effects in marine ecosystems," *Journal of Experimental Biology* , vol. 213, no. 6, pp. 881–893, Mar. 2010, doi: 10.1242/jeb.037523.

[18] S. Keerthikumar and S. Mathivanan, "Proteotypic Peptides and Their Applications," *Methods Mol. Biol.* , vol. 1549, pp. 101–107, 2017, doi: 10.1007/978-1-4939-6740-7_8.

[19] H. A. Ebhardt, A. Root, C. Sander, and R. Aebersold, "Applications of targeted proteomics in systems biology and translational medicine," *Proteomics* , vol. 15, no. 18, pp. 3193–3208, 2015, doi: https://doi.org/10.1002/pmic.201500004.

[20] B. Clarke, "Natural Selection and the Evolution of Proteins," *Nature* , vol. 232, no. 5311, p. 487, Aug. 1971, doi: 10.1038/232487a0.

[21] L. Mularoni, A. Ledda, M. Toll-Riera, and M. M. Albà, "Natural selection drives the accumulation of amino acid tandem repeats in human proteins," *Genome Res.* , vol. 20, no. 6, pp. 745–754, Jun. 2010, doi: 10.1101/gr.101261.109.

[22] D. Kültz, D. Fiol, N. Valkova, S. Gomez-Jimenez, S. Y. Chan, and J. Lee, "Functional genomics and proteomics of the cellular osmotic stress response in 'non-model' organisms," *J. Exp. Biol.* , vol. 210, no. Pt 9, pp. 1593–1601, May 2007, doi: 10.1242/jeb.000141.

[23] D. Kültz, J. Li, D. Paguio, T. Pham, M. Eidsaa, and E. Almaas, "Population-specific renal proteomes of marine and freshwater three-spined sticklebacks," *Journal of Proteomics* , vol. 135, pp. 112–131, Mar. 2016, doi: 10.1016/j.jprot.2015.10.002.

[24] B. A. Sardella and C. J. Brauner, "The Osmo-respiratory Compromise in Fish: The Effects of Physiological State and the Environment," in *Fish Respiration and Environment* , CRC Press, 2007, p. chapter 8.

[25] D. F. Fiol, E. Sanmarti, A. H. Lim, and D. Kültz, "A novel GRAIL E3 ubiquitin ligase promotes environmental salinity tolerance in euryhaline tilapia," *Biochimica et Biophysica Acta (BBA) - General Subjects* , vol. 1810, no. 4, pp. 439–445, Apr. 2011, doi: 10.1016/j.bbagen.2010.11.005.

[26] D. J. Speare, N. MacNair, and K. L. Hammell, "Demonstration of tank effect on growth indices of juvenile rainbow trout (Oncorhynchus mykiss) during an ad libitum feeding trial," *Am J Vet Res* , vol. 56, no. 10, pp. 1372–1379, Oct. 1995.

[27] Y.-W. Cui, H.-Y. Zhang, J.-R. Ding, and Y.-Z. Peng, "The effects of salinity on nitrification using halophilic nitrifiers in a Sequencing Batch Reactor treating hypersaline wastewater," *Sci Rep* , vol. 6, no. 1, p. 24825, Apr. 2016, doi: 10.1038/srep24825.

[28] S. Leary *et al.* , "AVMA Guidelines for the Euthanasia of Animals: 2020 Edition," p. 121, 2020.

[29] L. Root, A. Campo, L. MacNiven, P. Con, A. Cnaani, and D. Kültz, "Nonlinear effects of environmental salinity on the gill transcriptome versus proteome of Oreochromis niloticus modulate epithelial cell turnover," *Genomics* , vol. 113, no. 5, pp. 3235–3249, Sep. 2021, doi: 10.1016/j.ygeno.2021.07.016.

[30] L. K. Pino, B. C. Searle, J. G. Bollinger, B. Nunn, B. MacLean, and M. J. MacCoss, "The Skyline ecosystem: Informatics for quantitative mass spectrometry proteomics," *Mass Spectrom Rev* , vol. 39, no. 3, pp. 229–244, 2017, doi: 10.1002/mas.21540.

[31] J. Li, B. Levitan, S. Gomez-Jimenez, and D. Kültz, "Development of a Gill Assay Library for Ecological Proteomics of Threespine Sticklebacks (*Gasterosteus aculeatus*)," *Mol Cell Proteomics* , vol. 17, no. 11, pp. 2146–2163, Nov. 2018, doi: 10.1074/mcp.RA118.000973.

[32] S. Abbatiello *et al.* , "New Guidelines for Publication of Manuscripts Describing Development and Application of Targeted Mass Spectrometry Measurements of Peptides and Proteins.," *Molecular & cellular proteomics : MCP* , vol. 16, no. 3, pp. 327–328, Mar. 2017.

[33] M. Choi *et al.* , "MSstats: an R package for statistical analysis of quantitative mass spectrometry-based proteomic experiments," *Bioinformatics* , vol. 30, no. 17, pp. 2524–6, Sep. 2014, doi: 10.1093/bioinformatics/btu305.

[34] Y. Benjamini and Y. Hochberg, "Controlling the false discovery rate: A practical and powerful approach to multiple testing," *Journal of the Royal Statistical Society. Series B (Methodological)* , vol. 57, no. 1, pp. 289–300, 1995.

[35] D. Szklarczyk *et al.* , "STRING v11: protein–protein association networks with increased coverage, supporting functional discovery in genome-wide experimental datasets," *Nucleic Acids Res* , vol. 47, no. D1, pp. D607–D613, Jan. 2019, doi: 10.1093/nar/gky1131.

[36] L. Reiter *et al.* , "mProphet: automated data processing and statistical validation for large-scale SRM experiments," *Nat Methods* , vol. 8, no. 5, pp. 430–5, May 2011, doi: 10.1038/nmeth.1584.

[37] B. E. Davis *et al.* , "Consequences of temperature and temperature variability on swimming activity, group structure, and predation of endangered delta smelt," *Freshwater Biology* , vol. 64, no. 12, pp. 2156–2175, 2019, doi: 10.1111/fwb.13403.

[38] D. Kultz, J. Li, A. Gardell, and R. Sacchi, "Quantitative Molecular Phenotyping of Gill Remodeling in a Cichlid Fish Responding to Salinity Stress," *Molecular & Cellular Proteomics* , vol. 12, no. 12, pp. 3962–3975, Dec. 2013, doi: 10.1074/mcp.M113.029827.

[39] L. Root, A. Campo, L. MacNiven, P. Con, A. Cnaani, and D. Kultz, "A data-independent acquisition (DIA) assay library for quantitation of environmental effects on the kidney proteome of Oreochromis niloticus," *Molecular Ecology Resources* , vol. 21, no. 7, pp. 2486–2503, Oct. 2021, doi: 10.1111/1755-0998.13445.

[40] Evans, P. M. Piermarini, and K. P. Choe, "The Multifunctional Fish Gill: Dominant Site of Gas Exchange, Osmoregulation, Acid-Base Regulation, and Excretion of Nitrogenous Waste," *Physiological Reviews*

, vol. 85, no. 1, pp. 97–177, Jan. 2005, doi: 10.1152/physrev.00050.2003.

[41] J. Hiroi, S. D. McCormick, R. Ohtani-Kaneko, and T. Kaneko, "Functional classification of mitochondrion-rich cells in euryhaline Mozambique tilapia (Oreochromis mossambicus) embryos, by means of triple immunofluorescence staining for Na+/K+-ATPase, Na+/K+/2Cl- cotransporter and CFTR anion channel," *Journal of Experimental Biology* , vol. 208, no. 11, pp. 2023–2036, Jun. 2005, doi: 10.1242/jeb.01611.

[42] D. Kultz, K. Jurss, and L. Jonas, "Cellular and epithelial adjustments to altered salinity in the gill and opercular epithelium of a cichlid fish (Oreochromis mossambicus)," *Cell Tissue Res* , vol. 279, no. 1, pp. 65–73, Jan. 1995, doi: 10.1007/BF00300692.

[43] M. Inokuchi, J. Hiroi, S. Watanabe, P.-P. Hwang, and T. Kaneko, "Morphological and functional classification of ion-absorbing mitochondria-rich cells in the gills of Mozambique tilapia," *Journal of Experimental Biology* , vol. 212, no. 7, pp. 1003–1010, Apr. 2009, doi: 10.1242/jeb.025957.

[44] G. Bœuf and P. Payan, "How should salinity influence fish growth?," *Comparative Biochemistry and Physiology Part C: Toxicology & Pharmacology* , vol. 130, no. 4, pp. 411–423, Dec. 2001, doi: 10.1016/S1532-0456(01)00268-X.

[45] C. K. Tipsmark, J. P. Breves, A. P. Seale, D. T. Lerner, T. Hirano, and E. G. Grau, "Switching of Na+, K+-ATPase isoforms by salinity and prolactin in the gill of a cichlid fish," *J Endocrinol* , vol. 209, no. 2, pp. 237–244, May 2011, doi: 10.1530/joe-10-0495.

[46] J. G. Richards, J. W. Semple, J. S. Bystriansky, and P. M. Schulte, "Na+/K+-ATPase α-isoform switching in gills of rainbow trout (Oncorhynchus mykiss) during salinity transfer," *Journal of Experimental Biology* , vol. 206, no. 24, pp. 4475–4486, Dec. 2003, doi: 10.1242/jeb.00701.

[47] A. M. Gardell, J. Yang, R. Sacchi, N. A. Fangue, B. D. Hammock, and D. Kültz, "Tilapia (Oreochromis mossambicus) brain cells respond to hyperosmotic challenge by inducing myo-inositol biosynthesis," *Journal of Experimental Biology* , vol. 216, no. 24, pp. 4615–4625, Dec. 2013, doi: 10.1242/jeb.088906.

[48] A. A. Laskar and H. Younus, "Aldehyde toxicity and metabolism: the role of aldehyde dehydrogenases in detoxification, drug resistance and carcinogenesis," *Drug Metabolism Reviews* , vol. 51, no. 1, pp. 42–64, Jan. 2019, doi: 10.1080/03602532.2018.1555587.

[49] L. Zeng *et al.* , "Nuclear receptors NHR-49 and NHR-79 promote peroxisome proliferation to compensate for aldehyde dehydrogenase deficiency in C. elegans," *PLOS Genetics* , vol. 17, no. 7, p. e1009635, Jul. 2021, doi: 10.1371/journal.pgen.1009635.

[50] M. B. Rosen *et al.* , "Gene Expression Profiling in Wild-Type and PPARα-Null Mice Exposed to Perfluorooctane Sulfonate Reveals PPARα-Independent Effects," *PPAR Res* , vol. 2010, p. 794739, 2010, doi: 10.1155/2010/794739.

[51] T. Yamaguchi, M. Gi, M. Fujioka, Y. Tago, A. Kakehashi, and H. Wanibuchi, "A chronic toxicity study of diphenylarsinic acid in the drinking water of C57BL/6J mice for 52 weeks," *J Toxicol Pathol* , vol. 32, no. 3, pp. 127–134, 2019, doi: 10.1293/tox.2018-0067.

[52] U. O. Edet and S. P. Antai, "Correlation and Distribution of Xenobiotics Genes and Metabolic Activities with Level of Total Petroleum Hydrocarbon in Soil, Sediment and Estuary Water in the Niger Delta Region of Nigeria," *Asian Journal of Biotechnology and Genetic Engineering* , pp. 1–11, Jun. 2018.

[53] D. Kültz and H. Onken, "Long-term acclimation of the teleost Oreochromis mossambicus to various salinities: two different strategies in mastering hypertonic stress," *Marine Biology* , vol. 117, no. 3, pp. 527–533, Nov. 1993, doi: 10.1007/BF00349328.

[54] S. Fridman, K. J. Rana, and J. E. Bron, "Morphological and ultrastructural characterization of iono-regulatory cells in the teleost oreochromis niloticus following salinity challenge combining complementary

confocal scanning laser microscopy and transmission electron microscopy using a novel prefixation immunogold labeling technique," *Microscopy Research and Technique* , vol. 76, no. 10, pp. 1016–1024, 2013, doi: https://doi.org/10.1002/jemt.22262.

[55] T. H. Lee, P. P. Hwang, Y. E. Shieh, and C. H. Lin, "The relationship between 'deep-hole' mitochondria-rich cells and salinity adaptation in the euryhaline teleost, Oreochromis mossambicus," *Fish Physiology and Biochemistry* , vol. 23, no. 2, pp. 133–140, Aug. 2000, doi: 10.1023/A:1007818631917.

[56] M. Inokuchi and T. Kaneko, "Recruitment and degeneration of mitochondrion-rich cells in the gills of Mozambique tilapia Oreochromis mossambicus during adaptation to a hyperosmotic environment," *Comparative Biochemistry and Physiology Part A: Molecular & Integrative Physiology* , vol. 162, no. 3, pp. 245–251, Jul. 2012, doi: 10.1016/j.cbpa.2012.03.018.

[57] Karnaky, "Structure and Function of the Chloride Cell of Fundulus heteroclitus and Other Teleosts1," *American Zoologist* , vol. 26, no. 1, pp. 209–224, Feb. 1986, doi: 10.1093/icb/26.1.209.

[58] K. J. Karnaky Jr, S. A. Ernst, and C. W. Philpott, "Teleost chloride cell. I. Response of pupfish Cyprinodon variegatus gill Na,K-ATPase and chloride cell fine structure to various high salinity environments.," *Journal of Cell Biology* , vol. 70, no. 1, pp. 144–156, Jul. 1976, doi: 10.1083/jcb.70.1.144.

[59] P. Elumalai *et al.* , "The Role of Lectins in Finfish: A Review," *Reviews in Fisheries Science & Aquaculture* , vol. 27, no. 2, pp. 152–169, Apr. 2019, doi: 10.1080/23308249.2018.1520191.

[60] S. Hirose, T. Kaneko, N. Naito, and Y. Takei, "Molecular biology of major components of chloride cells," *Comparative Biochemistry and Physiology Part B: Biochemistry and Molecular Biology* , vol. 136, no. 4, pp. 593–620, Dec. 2003, doi: 10.1016/S1096-4959(03)00287-2.

[61] J. C. Tsai and P. P. Hwang, "Effects of wheat germ agglutinin and colchicine on microtubules of the mitochondria-rich cells and Ca2+ uptake in tilapia (Oreochromis mossambicus) larvae.," *Journal of Experimental Biology* , vol. 201, no. 15, pp. 2263–2271, Aug. 1998, doi: 10.1242/jeb.201.15.2263.

[62] J. C. Tsai and P. P. Hwang, "The wheat germ agglutinin binding sites and development of the mitochondria-rich cells in gills of tilapia (Oreochromis mossambicus)," *Fish Physiology and Biochemistry* , vol. 19, no. 1, pp. 95–102, Jul. 1998, doi: 10.1023/A:1007766531264.

[63] G. G. Goss, S. Adamia, and F. Galvez, "Peanut lectin binds to a subpopulation of mitochondria-rich cells in the rainbow trout gill epithelium," *American Journal of Physiology-Regulatory, Integrative and Comparative Physiology* , vol. 281, no. 5, pp. R1718–R1725, Nov. 2001, doi: 10.1152/ajpregu.2001.281.5.R1718.

[64] N. V. Grishin, "Estimation of the number of amino acid substitutions per site when the substitution rate varies among sites," *J Mol Evol* , vol. 41, no. 5, pp. 675–679, Nov. 1995, doi: 10.1007/BF00175826.

Data Accessibility Statement:

All proteomics data and metadata have been deposited and are publicly accessible at the following repositories MassIVE (MSV000085745) and ProteomeXchange (PXD020364) and ProteomeXchange (PXD020064) for all DDA data, and PanoramaPublic (https://panoramaweb.org/lr03.url) for all DIA data (including the DIA assay library).

Tables:

Table 1: CS_{max} during salinity increase and constant high salinity over time

CS_{max} at different rates of salinity increase

Rate	**CS_{max}**
6 g/kg/day	114.6 g/kg
8 g/kg/day	117.0 g/kg
12 g/kg/day	106.8 g/kg

24 g/kg/day	69.0 g/kg
32 g/kg/day	32.0 g/kg
CS_{max} over time at constant salinity	**CS_{max} over time at constant salinity**
salinity	**CS_{max}**
75 g/kg	not reached at 10 wks
85 g/kg	559 hrs
95 g/kg	326 hrs
105 g/kg	263 hrs

Figures:

Figure 1: Survival and organismal phenotypes during hypersalinity acclimation. a) Blood osmolality values for five 14-day acclimations after 24 hours at the target salinity (n=6 except at 75g/kg with n=4) and following extended exposure for 12 weeks (75g/kg, n=8) and at MP (85/105g/kg, n=6). **b)** Body condition for the same treatments as **c** . Letters in C and D were assigned using a post-hoc Tukey test following one-way ANOVA.

Figure 2: Growth and feeding during 12-week exposure to 75g/kg salinity. a) Size comparison of smallest and largest fish in the freshwater and 75g/kg treatment at the end of the experiment. **b)** Weight gain for FW control and at 75g/kg, with comparison between treatments. Significance was determined using Kruskal-Wallis test by ranks with "ns"- not significant, "*"- $p<0.05$, "**"- $p<0.005$, "***"- $p<0.0005$. **c)** Percent of fish body weight consumed daily over the course of the experiments, with weekly weighing identified by dashed vertical lines.

Figure 3 : Salinity effects on the gill proteome for five treatments. **a)** Volcano plots for each treatment with log2(Fold Change) plotted against log10(p-value). n=8 for 85 and 105g/kg 14-day acclimation and 75g/kg extended treatment, and n=6 for extended 85 and 105g/kg treatments. Significantly upregulated proteins are plotted in red with the total number of sig. upregulated proteins labelled, and significantly downregulated proteins are in blue. **b)** Overlap in all significantly regulated proteins between five treatments with the number of proteins in each segment labelled. **c)** Top significantly regulated proteins with the FC difference with controls shown. Redder boxes are more highly upregulated while bluer boxes are more highly downregulated.

Figure 4: STRING network showing all proteins which were significantly regulated in all treatments. Nodes represent one STRING protein ID and edges represent a connection based on protein-protein

interactions including known or predicted interactions based on published literature. Solid lines connect all members of one cluster, while dashed lines indicate connections that are not strong enough to be included in the same cluster based on a Markov Cluster inflation factor of 3. Central members of the Electron Transport Chain (red), glycolysis (green), and citric acid cycle (yellow) are indicated, along with specific proteins labelled. Insets used to more clearly display protein names.

Figure 5: STRING networks for pejus and pessimum stress stages and network; a) Networks with more than three nodes for all significantly regulated proteins found in the 12-week exposure to 75g/kg salinity representing pejus level salinity stress. Protein names in red were upregulated, those in blue were downregulated, and those outlined in red were upregulated in this treatment while being significantly downregulated in extended exposures to MP at 85g/kg and/or 105g/kg.**b)** Networks with more than three nodes for significantly regulated proteins found in all four pessimum level salinity stress treatments (14-day acclimation and extended exposure to 85g/kg and 105g/kg). Legend indicates the evidence used to connect protein nodes in each network.

Supplementary figures:

Supplementary figure 1: Salinity exposure protocols used to determine collect samples at relevant salinity-level/duration points before LER. To determine CS_{MAX}, salinity was raised at five different rates of change per day (32, 24, 12, 8, and 6g/kg/day) until LER. To determine CS_{MAX} over time at hypersalinity, salinity was increased at a rate of 6g/kg/day to three target salinity levels (85, 95, and 105g/kg) followed by continuous exposure at target salinity until LER. To assess physiological and molecular function at hypersalinity before LER, salinity was raised to four target levels (21g/kg, 55g/kg, 85g/kg, and 105g/kg) over14 days and samples collected following 24 hours at the final salinity. To assess the long-term impacts of hypersalinity below the critical salinity threshold, fish were acclimated from FW to 75g/kg at 6g/kg/day over 14 days followed by maintenance at the final salinity for 10 weeks for a 12 week acclimation in total. Samples used for proteomic analysis, chosen as representative of points above and below the critical salinity threshold, are circled in red.

Supplementary figure 2 : Properties of a *O. mossambicus*gill epithelium DIA assay library relative to the corresponding raw spectral library. The initial spectral library (SL) represents over 16,000 proteins, 139,000 precursors, and 864,000 transitions. Ten QC filters were applied to create the DIA assay library containing 3024 proteins (A), 13,847 peptides (B) and precursors (C), and 68,586 transitions (D). Most proteins are represented by at least 2 diagnostic peptides. The remainder (825) was identified by at least 2 unique peptides but only 1 remains after applying all DIA QC filters. The initial bar labeled SL depicts data for the raw spectral library and final bar (step 10) depicts data for the DIA assay library. Library filtration steps one to six are explained in the text. (E), Frequency distributions of fragment ion types represented in the final DIA assay library. b+ ions are fragments which extend from the N-terminus of the peptide and y+ ions extend from the C-terminus i.e. a 3 fragment ion denominator member contains the first three peptides for a b+ ion and the last three for a y+ ion. (F), Frequency distribution for the number of peptides per protein in the DIA assay library. The data were generated with Skyline 20.0 (MacCoss Lab., University of Washington).

Supplementary figure 3 : Quality control parameters summarized for all samples in five treatments analyzed in this study. A) The mean mass error (ppm) for all transitions present in the final assay library in the 14-day 85g/kg treatment. Other treatments shown are 14-day 105g/kg (E), extended 85g/kg (I), extended 105g/kg (M), and 12-week 75g/kg (Q). B) Retention time for the 14-day 85g/kg treatment. reproducibility for all transitions in all samples analyzed in this study was very high ($r^2 = 1.0$). Other treatments shown are 14-day 105g/kg (F), extended 85g/kg (J), extended 105g/kg (N), and 12-week 75g/kg (R). C) Fold change (FC) and coefficient of variation (CV) depending on number of biological replicates at a statistical power of 0.8 and false discovery rate (FDR) of 1% in the 14-day 85g/kg treatment. Other treatments shown are 14-day 105g/kg (G), extended 85g/kg (K), extended 105g/kg (O), and 12-week 75g/kg (S). D) mProphet Q values for all transitions in all samples in the 14-day 85g/kg treatment. Other treatments shown are 14-day 105g/kg (H), extended 85g/kg (L), extended 105g/kg (P), and 12-week 75g/kg (T). Figures were generated with Skyline 20.0 (including MSstats and mProphet) software (MacCoss Lab., University of Washington).

Supplementary figure 4: Alignment and distance tree of full uncharacterized protein sequence and one repeat of the sequence. A) Alignment of the full sequence of the uncharacterized protein LOC100699110 - X1 with all named proteins in the top 100 blastp results based on E-value using the non-redundant protein sequence database of the NCBI and no specified organism. B) Alignment of the 143 amino acid (AA) repeat segment using the same parameters as in A. C) Distance tree of results from A based on BLAST computed pairwise alignment with evolutionary distance modeled as the expected fraction of AA substitutions per site based on the fraction of mismatched AAs in the region following [64]. D) Distance tree of results for 143 AA repeat results. E) Beginning section of the amino acid sequence showing peptide coverage from the DIA assay library. Repeat AA segment is highlighted.

Supplementary tables:

Supplementary table 1 : Fold Change and p-values for all proteins in all treatments

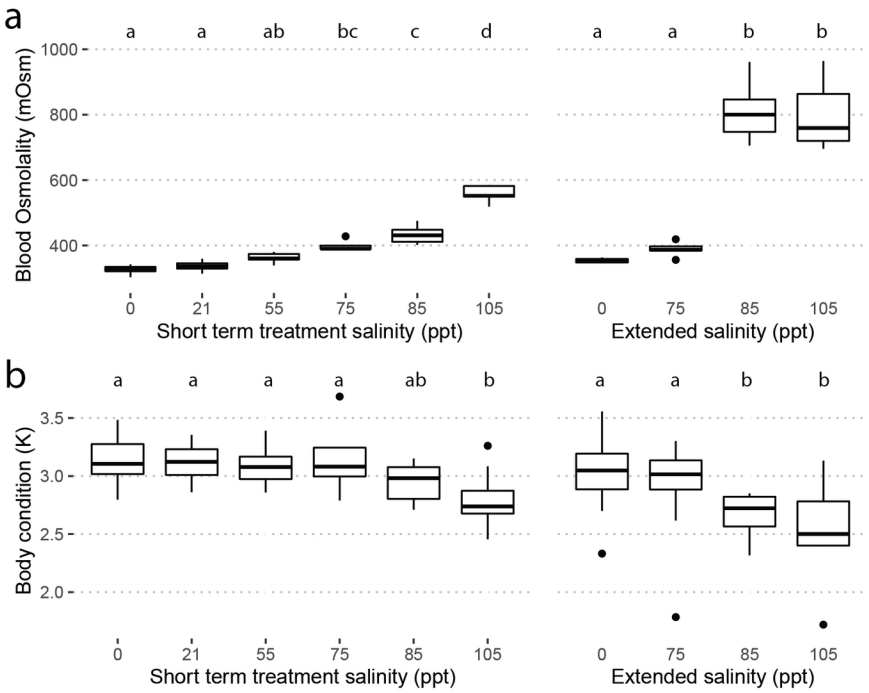

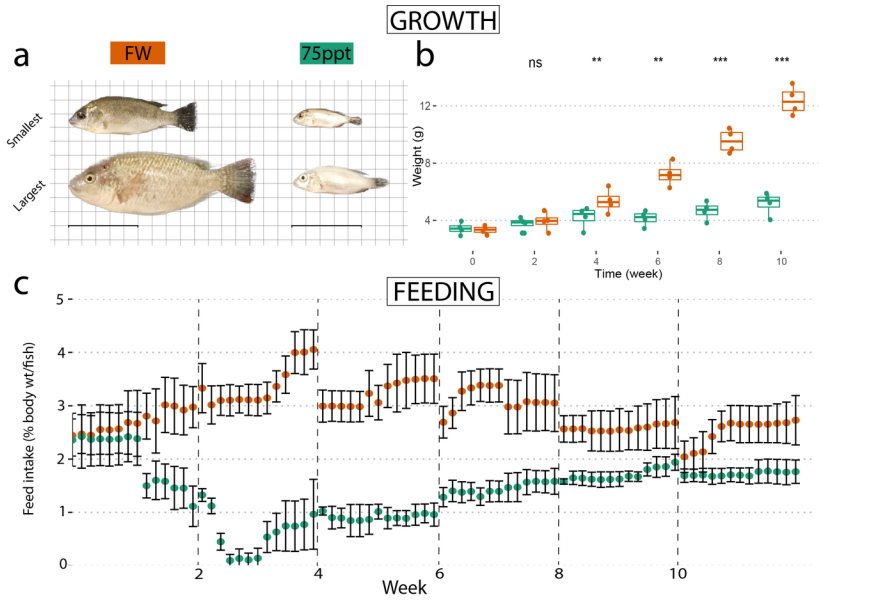

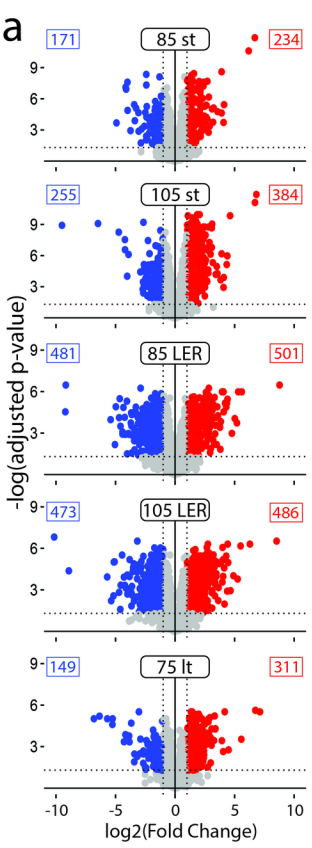

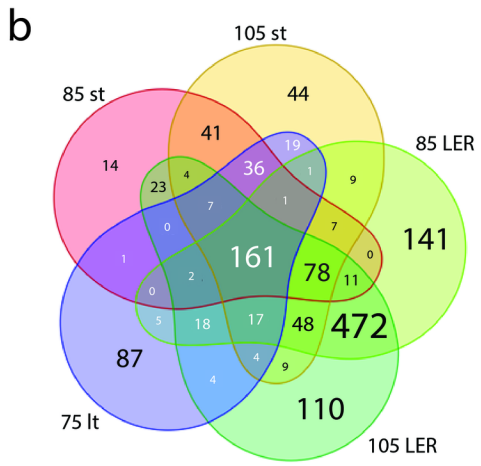

c

	85 st	105 st	85 LER	105 LER	75 lt	mean
inositol monophosphatase 1	6.2	6.7	8.8	8.5	7.1	7.5
solute carrier family 12 member 2	6.7	6.8	5.6	6.3	6.7	6.4
solute carrier family 12 member 3	4.1	4.4	4.1	4.4	4.5	4.3
phosphoglycerate mutase 1	3.9	4.6	4.3	4.5	4.2	4.3
neuronal membrane glycoprotein M6−b	3.9	4.3	2.6	3.3	5.6	3.9
pinin	4.1	4.1	3.5	3.6	4.0	3.9
enolase	2.9	3.5	5.0	4.9	0.9	3.5
acidic amino acid decarboxylase GADL1	1.5	4.1	5.2	5.2	NP	3.2
E3 ubiquitin−protein ligase rnf213−β	0.7	1.8	5.3	5.5	0.0	2.7
microfibril−associated glycoprotein 4	−4.9	NP	−3.0	−2.9	−3.9	−2.9
glutathione S−transferase A	−2.4	−2.3	−2.8	−3.5	−5.2	−3.2
anterior gradient protein 2 homolog	−1.8	−2.1	−5.4	−5.7	−2.9	−3.6
mucin−5AC	−3.0	−2.7	−3.6	−3.5	−5.3	−3.6
rhamnose−binding lectin	−3.4	NP	−4.0	−4.6	−6.3	−3.7
band 3 anion exchange protein	−4.2	−4.2	−4.0	−3.8	−2.2	−3.7
catenin δ−1	−2.0	−2.3	−9.2	−8.9	1.3	−4.2
Na /K −transporting ATPase subunit α−1	−3.4	−4.2	−5.0	−5.1	−4.0	−4.4
apolipoprotein D	−4.0	−4.7	−5.0	−5.4	−2.6	−4.4
IgGFc−binding protein	−4.1	−6.5	−4.6	−4.4	−5.7	−5.1
uncharacterized protein LOC100699110	−4.0	−9.5	−9.2	−10.2	−6.8	−7.9

−10 −5 0 5 10